Simulation of the Forming of a Superelastic Anchoring Stent and its Deployment in the Coronary Vein

Milton A. DeHerrera, Ph.D. and Wei Sun, Ph.D
Edwards Lifesciences LLC
1 Edwards Way
Irvine, CA 92614
USA

Abstract: Mitral valve regurgitation (MR) occurs when a flaw in the mitral valve causes backflow of blood into the left atrium. It is possible to reduce the amount of MR by reshaping the mitral annulus which, in turn, changes the configuration of the valve leaflets. A new percutaneously-delivered device which induces this reshaping is currently under development at Edwards Lifesciences. The device, which is placed in the coronary sinus (CS), is essentially a spring with anchoring stents at each end. This study examines the mechanical behavior of one of the anchoring stents, from its forming from a small diameter tube to its deployment into the coronary sinus. The anchoring stent is modeled using the ABAQUS Superelastic constitutive model, and the CS is modeled using a hyperelastic constitutive model.

Keywords: ABAQUS Explicit, ABAQUS Standard, Cardiovascular Therapy, Constitutive Model, Contact, Fatigue, Fatigue Life, Forming,, Hyperelasticity, Implantable Medical Device, Mass Scaling, Minimally Invasive Surgery, Mitral Valve Repair, NiTinol, Percutaneous Devices, Ogden Model, Percutaneous Stent Delivery, Superelasticity, Tissue Modeling, UMAT, VUMAT

1. Introduction

This paper analyzes the stresses and strains in the Proximal Anchor for a Mitral Repair Device being developed at Edwards Lifesciences. We aim for a quantitative comparison between modeling a device embedded in a rigid enclosure versus one in a deformable enclosure. The initial phase of the study consists of numerical simulation of the expansion-annealing process used to expand the anchoring stent from its initial tube outer diameter (OD) of 2.2mm to a final OD of about 15.5mm. The second phase consists of simulating crimping of the stent to a smaller OD with a subsequent cyclic radial load to help evaluate pulsatile fatigue behavior in the stent. The final phase analyzes the behavior of the stent when deployed in a hyperelastic tube that mimics the Coronary Sinus (CS), including a cycled pressure loading.

2. Overview of initial FEA model

The proximal anchor can be thought of as an elastic lattice, deriving its strength from the joints and bending action of component struts. Because of the lack of symmetry in this part, the entire anchor has been modeled. The initial CAD geometry for the electropolished anchor was provided (Figure 1) and subsequently imported into a pre-processor, where it evolved into a flat 2D mesh. Through a simple trigonometric transformation, this flat mesh was converted into a cylindrical mesh representing the anchor OD, with removal of all redundant coincident nodes completing the meshing task. A final 3D mesh comprised of hexahedral elements was generated through a radially inward normal sweep from the 2D cylindrical mesh through a distance equal to the tube thickness.

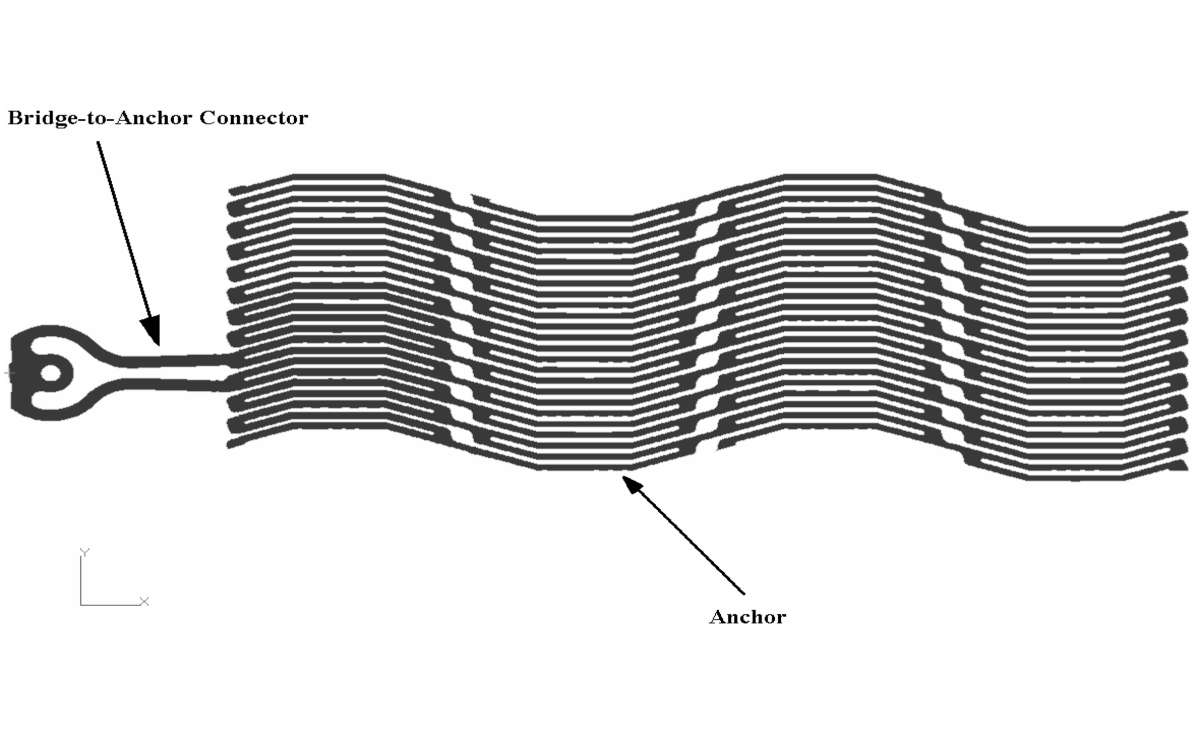

Figure 1. Original flat CAD geometry used to define Proximal Anchor.

3. Analysis model

The analysis was run with ABAQUS/Explicit release 6.6 EF-1 on a 16-CPU Linux cluster running SuSE 9.0. We used C3D8R hexahedral elements for deformable domains and M3D4R membrane elements for the rigid domains. The main body of the undeformed anchor model is approximately 21mm long, and 26mm long if we include the Bridge-to-Anchor connector. The topological FEA description of the deformable part model is as follows:

ELSET	#/type of elements	# of nodes
Anchor	114220/C3D8R	163596
Coronary Sinus (CS)	43200/C3D8R	52272

In this study, we have used the ABAQUS Superelastic model for the anchor and a hyperelastic Ogden model for the coronary sinus (CS). Parameters for the superelastic material model were obtained from dogbone samples tested in our facility. Data for the Ogden model was generated by curve-fitting data from (Stooker, et al 2003). The input parameters required for this material model are described in the next section. Figure 2 illustrates the undeformed 3D solid mesh used in this study.

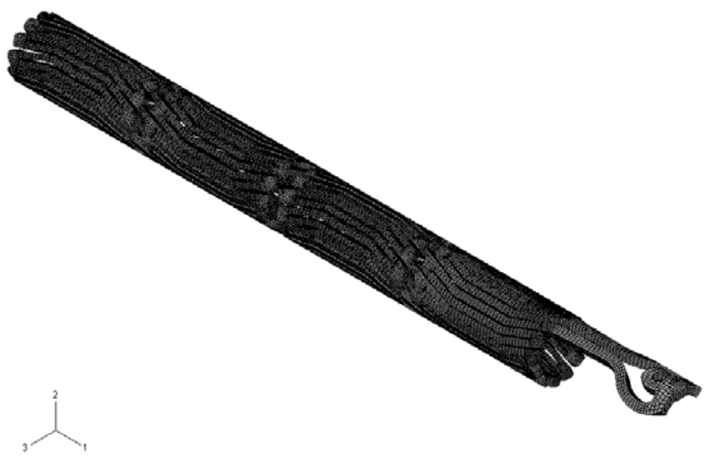

Figure 2. Undeformed mesh of proximal anchor model.

4. The ABAQUS superelastic model

The ABAQUS Superelastic model is based on the work of (Auricchio, et al 1997), (Lubliner, et al 1996), with extensions by (Rebelo, 2002). For an isothermal analysis, the model can be defined by a stress-strain curve and “breakpoint” stresses shown on Figure 3 below. A more detailed discussion is given in (DeHerrera, 2004).

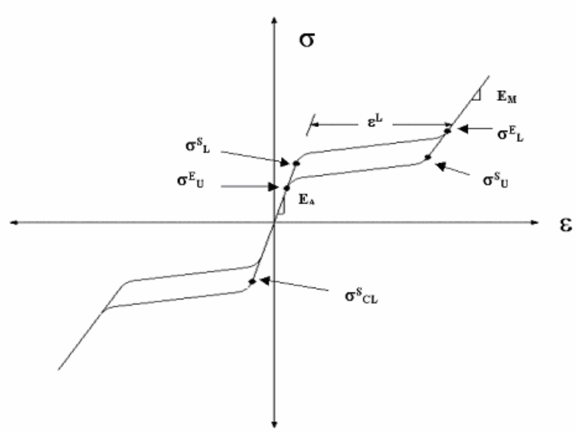

Figure 3. Illustration of the ABAQUS Superelastic material model nomenclature.

The primary mechanical inputs to this model are two modulii of Elasticity, two Poisson ratios, a plateau transformation strain, and five stress breakpoints. Below is a list of the input parameters required to run this model in ABAQUS:

E_A = Austenitic Elastic Modulus
ν_A = Austenitic Poisson's ratio
E_M = Martensitic Elastic Modulus
ν_M = Martensitic Poisson's ratio
ε^L = Transformation strain
$(\delta\sigma/\delta T)_L$ = Loading $(\delta\sigma/\delta T)$
σ^S_L = Start of transformation stress during loading
σ^E_L = End of transformation stress during loading
T_0 = Reference temperature
$(\delta\sigma/\delta T)_U$ = Unloading $(\delta\sigma/\delta T)$
σ^S_U = Start of transformation stress during unloading
σ^E_U = End of transformation stress during unloading
σ^S_{CL} = Start of transformation stress during compressive loading

The input values for reference temperature T_0 , and the Classius-Clapeyron stress-temperature constants $(\delta\sigma/\delta T)_L$ and $(\delta\sigma/\delta T)_U$ are not as important if the analysis is done at T_0.

5. Hyperelastic model of the Coronary Sinus

There is a paucity of experimental data on the physical environment in the coronary sinus, and even less on its mechanical properties. The closest applicable human data we found was from a paper by (Stooker, et al, 2003) describing the pressure-diameter relationship in the Greater Saphenous Vein. We have chosen this data, in combination with the Ogden constitutive model to mechanically represent the coronary sinus. A typical Ogden model is of the form:

$$W = \sum_{i=1}^{N} \frac{2\mu_i}{a_i^2}(\lambda_1^{a_i} + \lambda_2^{a_i} + \lambda_3^{a_i} - 3) \qquad (1)$$

where W is the strain energy density, μ_i and a_i are material constants and λ_i are the principal stretches. Because we are using ABAQUS/Explicit, a slight amount of compressibility equivalent to a $\nu = 0.499$ was enabled in the Ogden formulation. A separate quarter-tube model for the vein was used to generate the Ogden material parameters. Figure 4 shows a plot of diametric strain $\Delta D/D$ versus pressure from Stooker's data and from the Ogden curve fit results.

In the near future, as we get more experimental data, we intend to use more sophisticated tissue models such as Fung-type models (Sun et al, 2005).

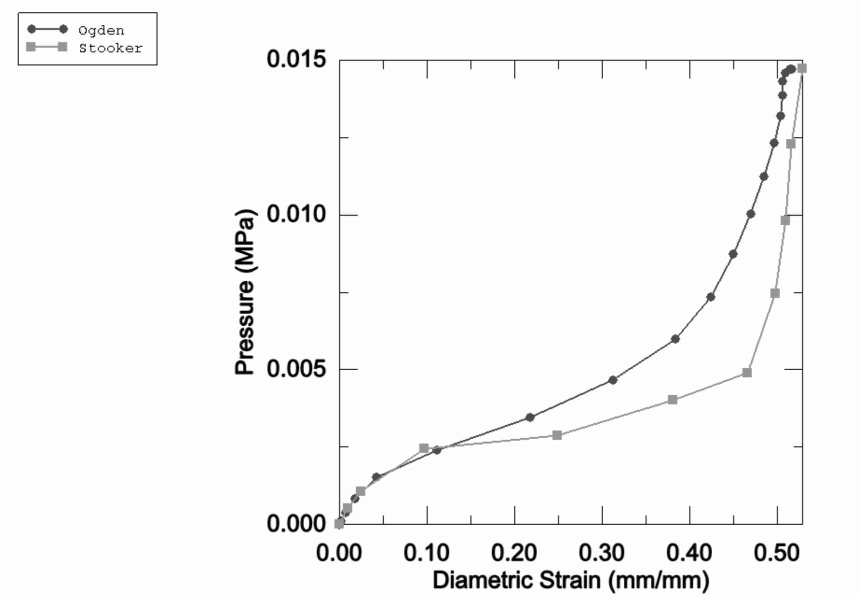

Figure 4. Comparison of Pressure vs Diametric Strain curves from (Stooker, 2003) with a curve-fitted Ogden model.

6. Simulation of expansion-annealing process for Proximal Anchor

The proximal anchor is Laser-cut from a 2.2mm OD Nitinol tube. The expansion to a 15mm ID is accomplished by applying a series of radial displacements to an inner forming surface in contact with the ID of the tube, followed by several annealing steps. The sequence and resulting maximum tensile strains SDV24 and LEP3 are shown on Figure 5 below.

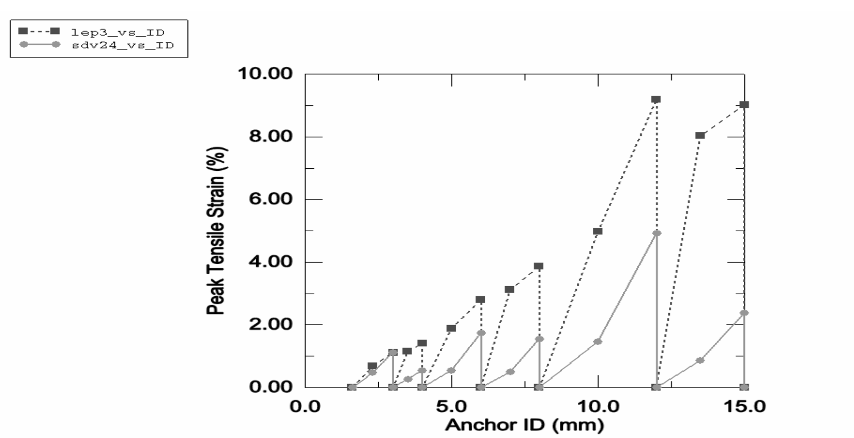

Figure 5. Comparison of peak tensile strains SDV24 and LEP3 during expansion/forming as a function of anchor ID.

It's important to note that, when annealing steps are applied during an analysis, the values of SDV24 and LEP3 (which tend to be nearly identical when ***anneal** is not used) are quite different. The SDV24 variable is the proper one to use for analyses of superelastic materials involving annealing.

7. Simulation of anchor crimping by a rigid surface

Before doing any analysis with tissue models, we want to study the crimping and fatigue-inducing loads using a rigid cylindrical surface. We should note that, even though we speak of a "rigid" surface, it is mechanically described by an elastic material law, albeit with an Elastic modulus much larger than the initial austenitic modulus (E_A) of the anchor.

Most stent type devices are oversized with respect to the vessel in which they are deployed, i.e., the device diameter is typically from 1 to 3mm larger than the vessel diameter. When a 15.5mm device is deployed in a 12mm diameter CS, its final OD will be somewhere between 12.5mm and 14mm, depending on the CS's compliance. In order to get an initial estimate of the tensile strains in the proximal anchor, the model is uniformly crimped from an initial OD of 15.5mm down to a final OD of 13.5mm. Figures 6 and 7 show the SDV24 (peak tensile strain) at the end of crimping and after adding an axial load to Bridge-to-Anchor connector, respectively. Figure 8 plots SDV21 (Martensitic fraction ξ) fields at the crimped + axial load configuration.

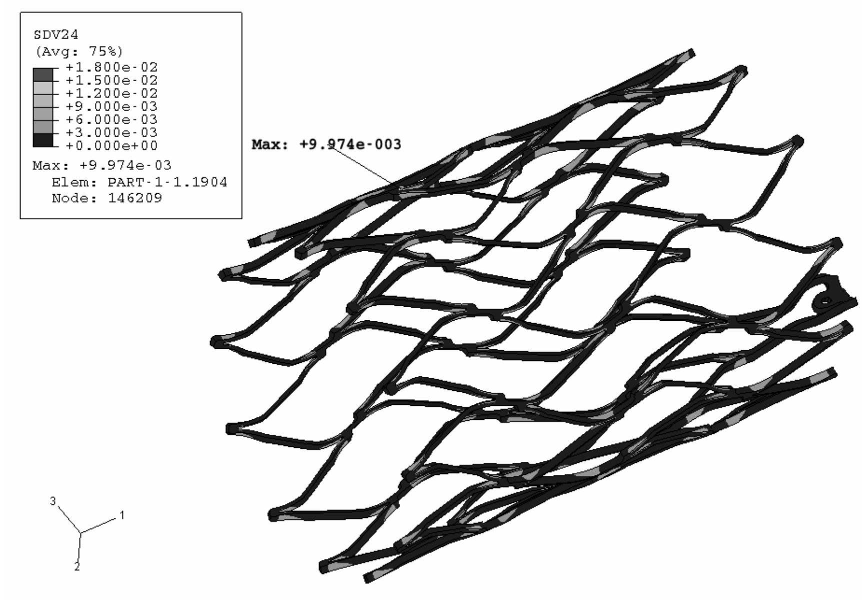

Figure 6. Peak tensile strain SDV24 in Proximal Anchor after crimping to an OD = 13.5mm.

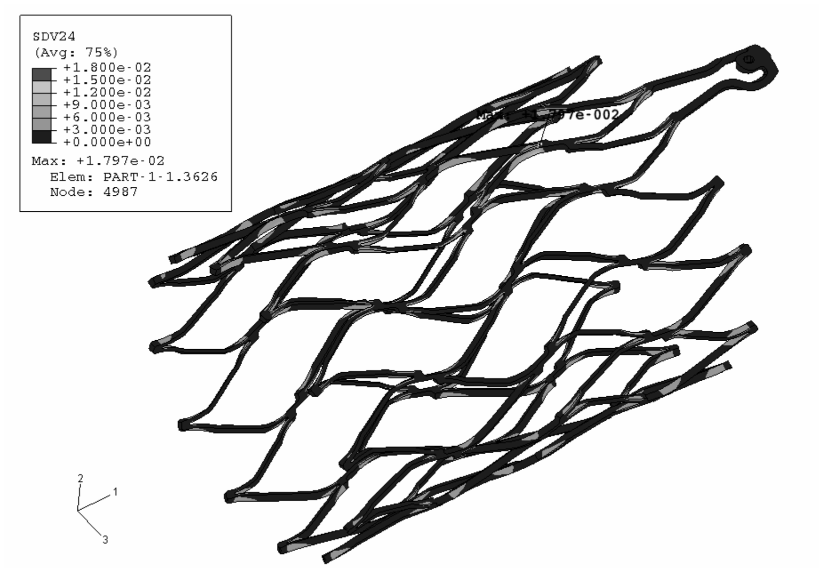

Figure 7. Peak tensile strain SDV24 in Proximal Anchor after crimping to an OD = 13.5mm and adding an axial load to Bridge-to-Anchor Connector.

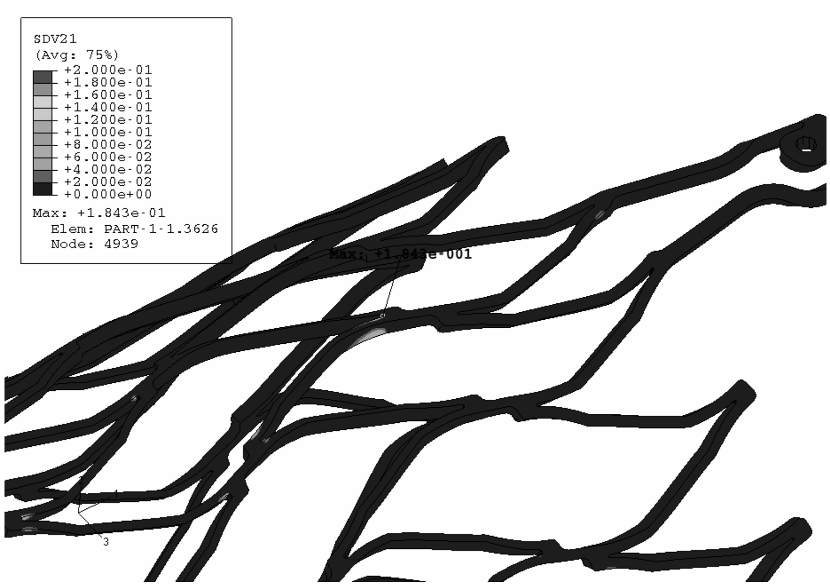

Figure 8. Closeup view of martensitic fraction ξ in Proximal Anchor after crimping to an OD = 13.5mm and adding an axial load to Bridge-to-Anchor Connector.

8. Mechanical fatigue analysis methodology: Goodman Plot/Diagram

When the Mitral Repair Device is implanted in the coronary sinus, it will be subjected to a pulsatile load that may or may not cause fatigue damage to the device. Quantitative studies of material fatigue often make use of a Goodman-Haigh plot/diagram, where the abscissa represents the mean stress or strain at a point and the ordinate represents the amplitude (or half-amplitude) of stress or strain at the same point. The distinction between a "Goodman plot" and a "Goodman diagram" is that the former is a plot of (mean,amplitude) stress/strain ordered pairs, and the latter also includes a Constant Life Curve, which plots the boundary beyond which fatigue failure is expected to occur. Because of the proprietary nature of the experimentally developed Constant Life curves, we will only present Goodman plots. In the first phase of this study, where the anchor displacement is being driven by a cylindrical rigid surface that can only impart motions in the radial direction, the displacement field can be adequately described by a mean rigid surface diameter and the displacement amplitude about that mean diameter. It is convenient, but by no means necessary, to use a sinusoidal function to describe the displacement amplitude variation about some mean diameter value. By studying changes in maximum tensile strain that occur in the anchor during such a cycle, fatigue effects can be evaluated via a Goodman plot/diagram.

Given a rigid surface with mean diameter D and displacement half-amplitude A, we use the notation "fat" or "thin" to denote the configurations $D_1 = D + A$ and $D_2 = D – A$, respectively. The mean maximum tensile strain in the anchor at a given node is calculated from the equation:

$$\varepsilon_{meanD} = \tfrac{1}{2}\,|\varepsilon_{fat} + \varepsilon_{thin}| \qquad (2)$$

where ε_{fat} and ε_{thin} are the maximum tensile strains at said node in the "fat" and "thin" configurations, respectively. Similarly, the half-amplitude $\Delta\varepsilon$ is given by:

$$\Delta\varepsilon = \tfrac{1}{2}\,|\varepsilon_{fat} - \varepsilon_{thin}| \qquad (3)$$

Strictly speaking, the above equations for ε_{meanD} and $\Delta\varepsilon$ are approximations. The reason is that the principal directions of ε_{fat} and ε_{thin} are not always coincident. However, a study conducted by the first author (DeHerrera, 2006) concluded that, given an applied radial displacement on this type of stent consistent with the human anatomy and considering the resulting strain levels, the error is small.

There are several ways of extracting data necessary to generate the Goodman points (ε_{meanD} , $\Delta\varepsilon$). We chose to output SDV24 at "fat" and "thin" configurations using the ABAQUS/Viewer **Report/Field Output/Unique Nodal** feature. The output files for each configuration were processed through a FORTRAN program that formed and sorted the Goodman points, and the data was imported back into ABAQUS/Viewer as xy-data. Because Goodman plots are sometimes difficult to read when there are tens of thousands of points, we occasionally find it convenient to plot a "Skyline" plot where all the Goodman points are placed in 200 bins of width *D*, where

$$D = [\max(\varepsilon_{meanD})]/200 \qquad (4)$$

9. Displacement-controlled fatigue study

The initial baseline geometry for crimping was obtained from the forming analysis in section 6 above, with an initial OD = 15.5mm. After crimping the anchor to an OD = 13.5mm, a sinusoidal radial displacement was applied through the rigid surface to simulate a cyclic load, allowing the extraction of the Goodman points (ε_{meanD} , $\Delta\varepsilon$). Figures 9 and 10 show the corresponding Goodman and Skyline plots for an anchor crimped to OD = 13.5mm with an applied cyclic radial displacement.

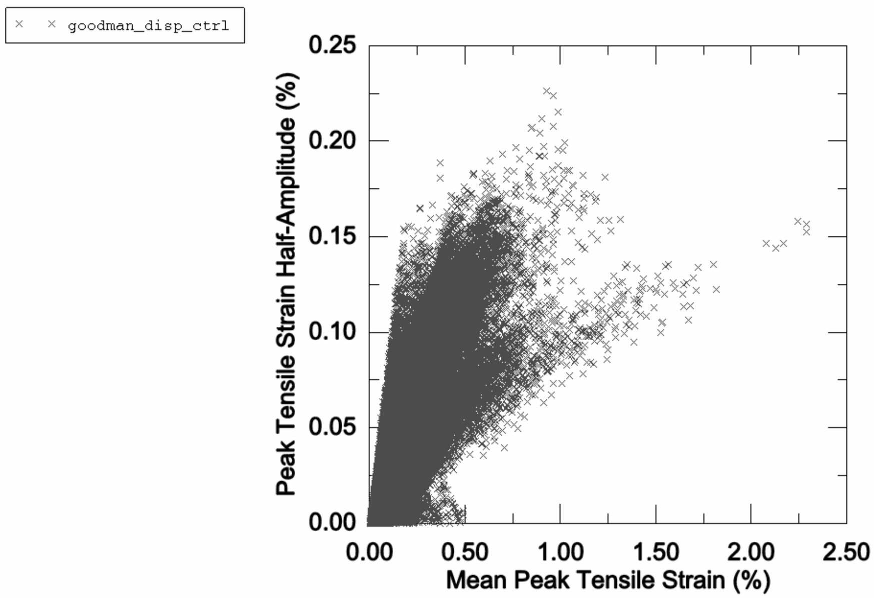

Figure 9. Displacement-controlled Goodman plot for a Proximal Anchor crimped to OD = 13.5mm with an added axial load to Bridge-to-Anchor Connector.

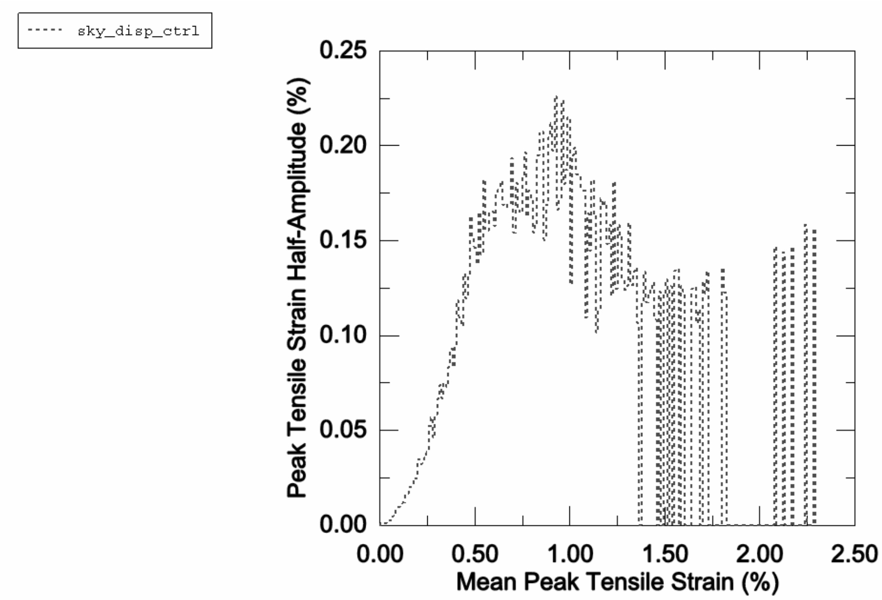

Figure 10. Displacement-controlled Goodman skyline plot for a Proximal Anchor crimped to OD = 13.5mm with an added axial load to Bridge-to-Anchor Connector.

10. Simulation of deployment in coronary vein and load-controlled fatigue study

A major objective of this study was to see how the anchoring stent deforms in a hyperelastic tube, in effect to see how it compares with the results from a rigid tube. In particular, we want to compare the Goodman plots from a "deformable" or load-controlled analysis with those from a "rigid" or displacement-controlled analysis. With respect to load boundary conditions in the Coronary Sinus, we have used a maximum pressure of 5mm Hg based on the work of (Ganong, 1971). For the minimum pressure, we used both 0mm Hg and -2mm Hg, although the latter is probably unrealizable.

As was done with the rigid case, the initial baseline geometry for crimping was obtained from the forming analysis in section 6. The analysis sequence was made up of the following steps:

1. Crimp anchor to an OD of 12mm, which is the ID of the hyperelastic tube representing the coronary sinus (see Figure 11).
2. Release the anchor into contacting the CS model (Figure 12).
3. Apply an axial load to account for the expanded device Bridge/spring load (Figure 13).
4. Apply an internal pressure to the CS model, starting a 0mm Hg, ramped down to -2.0mm Hg and ramped up to 5mm Hg

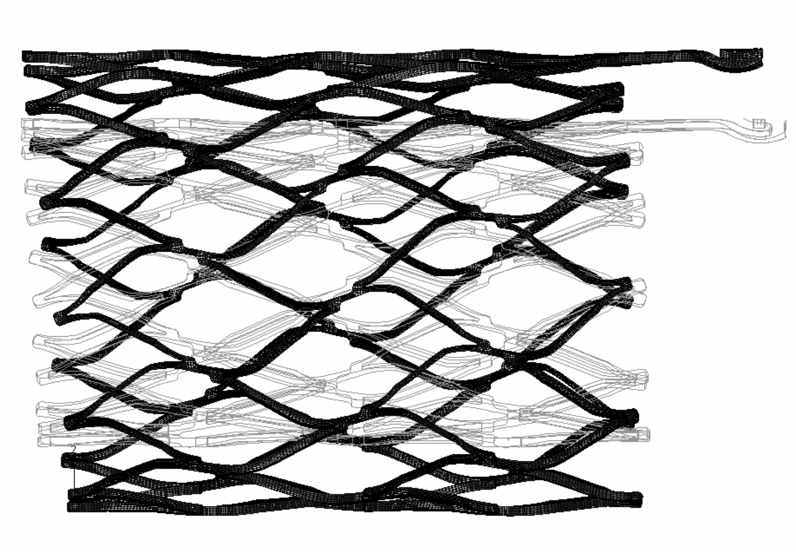

Figure 11. Deformed/undeformed plot of Proximal Anchor crimped to an OD = 13.5mm.

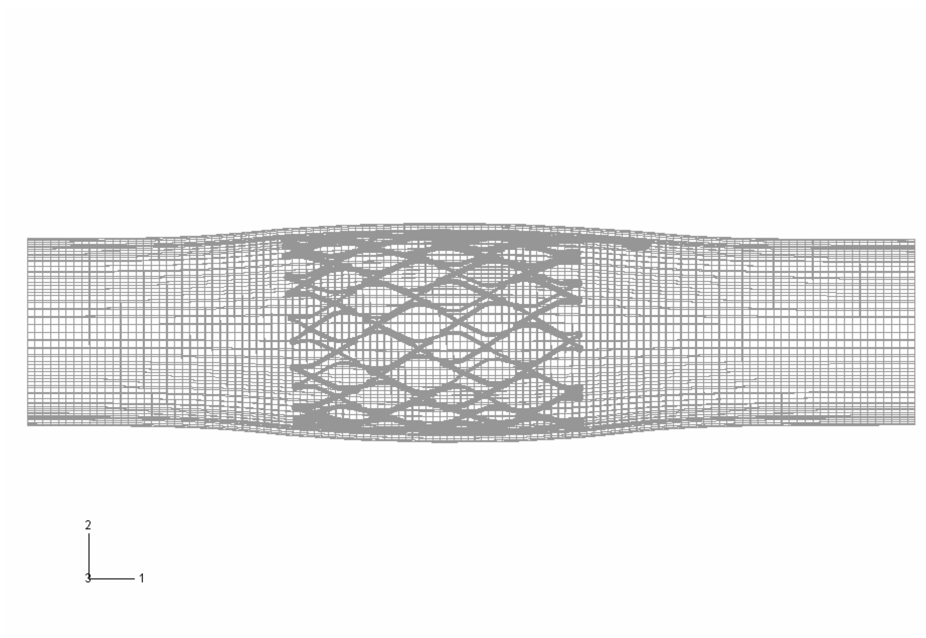

Figure 12. Deformed plot of Proximal Anchor and hyperelastic coronary sinus models after contact is established.

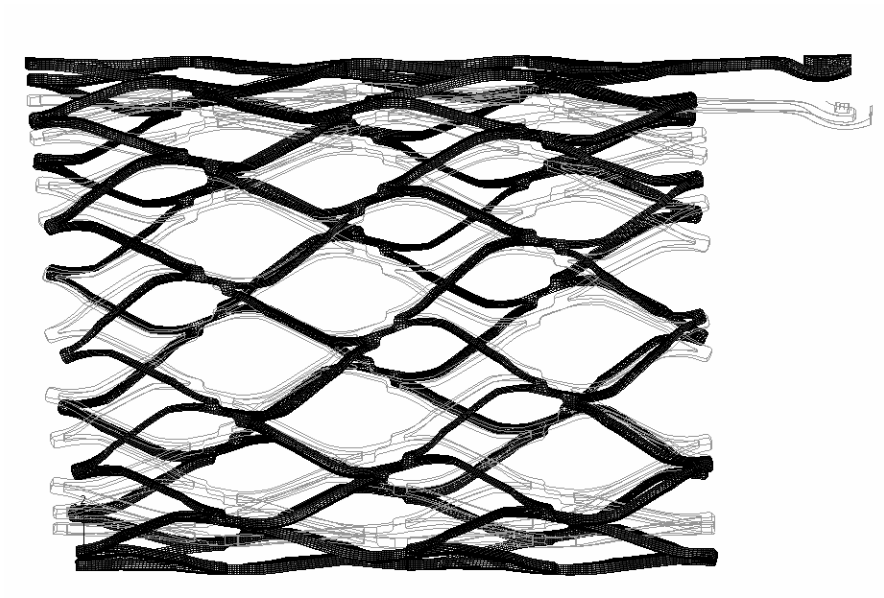

Figure 13. Deformed/undeformed plot of Proximal Anchor embedded in coronary sinus model after application of axial load to Bridge-to-Anchor connector.

After crimping the anchor to an OD = 13.5mm, two sets of pressure loading were applied to the inner surface of the coronary sinus model. Load set **load_ctrl_0** goes from P = (P_{min} , P_{max}) = (0, 5)mm Hg and **load_ctrl_1** goes from (P_{min} , P_{max}) = (-2, 5)mm Hg. Extraction of the Goodman points (ε_{meanD} , $\Delta\varepsilon$) follows a procedure similar to that used for the displacement-controlled study in section 9. Figure 14 shows the corresponding Goodman plot for both load cases. Finally, Figures 15 and 16 show all cases plotted simultaneously. It can be seen that the Goodman points generated from a load-controlled analysis have a much lower strain half-amplitude , which implies that the original displacement-controlled analysis using a rigid surface will give a conservative estimate of fatigue.

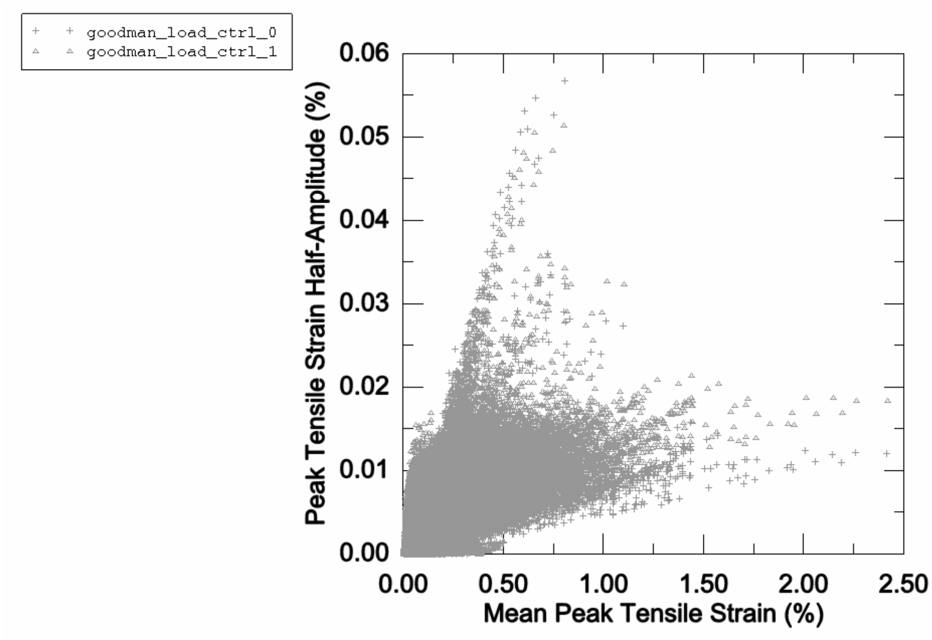

Figure 14. Goodman plots for load-controlled cases.

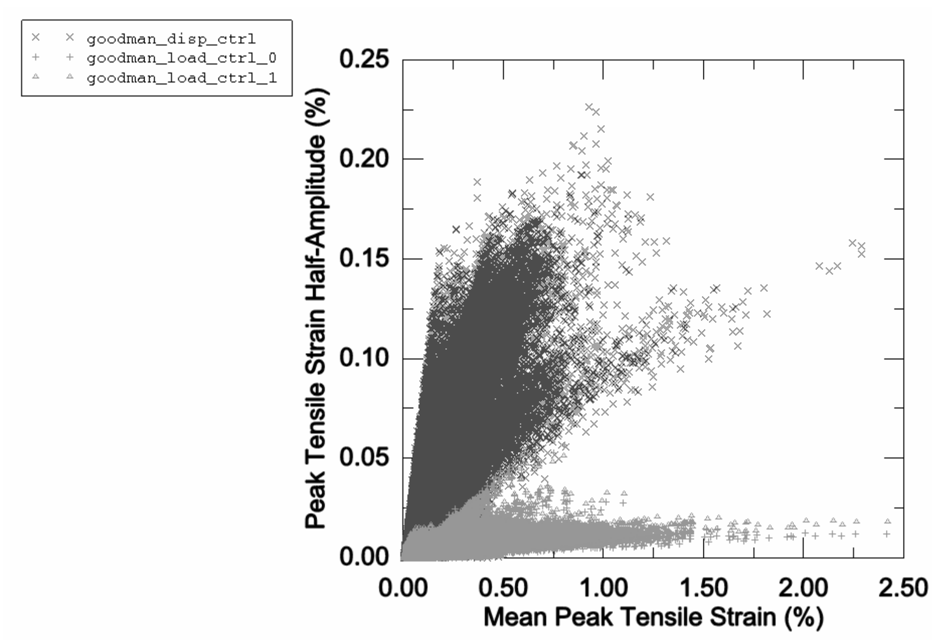

Figure 15. Goodman plots for all cases.

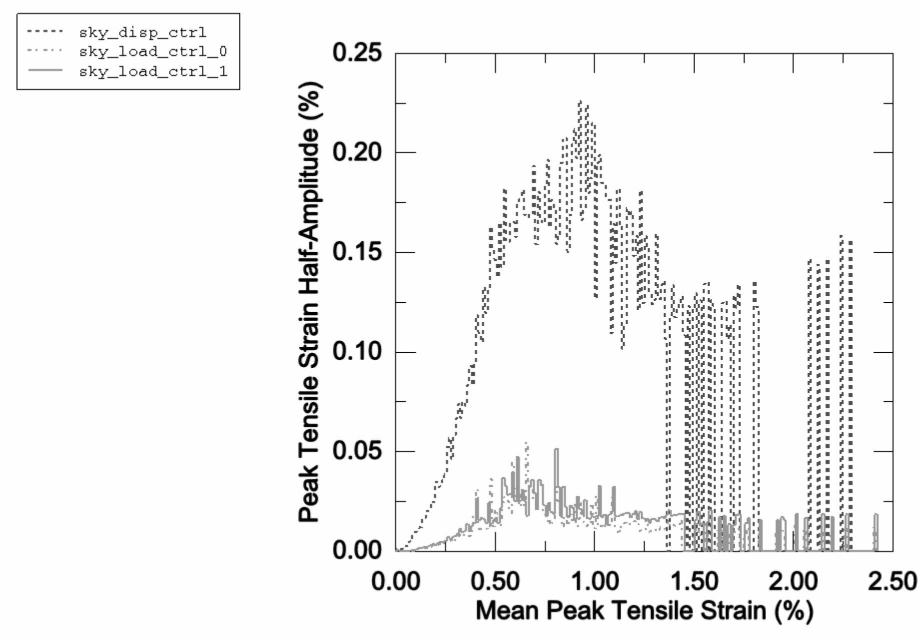

Figure 16. Goodman skyline plots for all cases.

11. Conclusions

A major objective of this study was to compare and evaluate the difference between modeling the anchoring stents in a rigid enclosure versus a deformable, hyperelastic enclosure. By examining the resulting Goodman plots for each case we conclude that the rigid surface driven model yields conservative results, the former giving half-strain amplitudes that are significantly higher. Further studies using better tissue models relying on human cadaver coronary sinus specimens are planned.

12. References

1. Auricchio, F. and R.L. Taylor "Shape-Memory Alloys: Modeling and Numerical Simulations of the Finite-Strain Superelastic Behavior." *Computational Methods in Applied Mechanics and Engineering* **143** (1997), 175-194

2. Auricchio, F., R.L. Taylor and J. Lubliner "Shape-Memory Alloys: Macromodelling and Numerical Simulations of the Superelastic Behavior." *Computational Methods in Applied Mechanics and Engineering* **146** (1997), 281-312

3. DeHerrera, M.A. "Computation of Mean Peak Strain and Peak Strain Amplitudes due to Cyclic Loading via Exact (Tensor) and Approximate (Scalar) Means." *Edwards Lifesciences Internal Memo(2006)*

4. DeHerrera, M. A. and N. Dang "Finite Element Analysis of a Percutaneous Stent-Mounted Heart Valve." *Proceedings of the ABAQUS Users' Conference, Boston, Massachusetts, June 2004, pp. 209 - 223.*

5. Ganong, William F. **Review of Medical Physiology**. Lange Medical Publications, 1971, pp 426-427.

6. Lubliner, J. and F. Auricchio "Generalized Plasticity and Shape-Memory Alloys." *International Journal of Solids and Structures* **33** (1996), 991-1003

7. Rebelo, N. *Private Communication,* (2002)

8. Stooker, W, M. Gök, P. Sipkema, H. Niessen, A. Baidoshvili, N. Westerhof, E. Jansen, C. Wildevuur an L. Eijsman "Pressure-Diameter Relationship in the Human Greater Saphenous Vein." *Annals of Thoracic Surgery* **76** (2003), pp. 1533-1538

9. Sun, W., M. Scott and M.S. Sacks, "Finite Element Implementation of a Fung Elastic Model for Planar Anisotropic Biological Materials," *Biomechanics and Modeling in Mechanobiology*, November 2005(2-3), pp. 190-199.

13. Acknowledgments

Drafts of this work were reviewed by Seung Yi, Chip Corso and Hengchu Cao of Edwards Lifesciences. The first author had valuable technical discussions with his former co-workers Mr. Mike LeDuc and assistance from Andrew Spain, both of Freudenberg-NOK General Partnership in New Hampshire, USA.